Nuclear Shp2 directs normal embryo implantation via facilitating the ERα tyrosine phosphorylation by the Src kinase

Hao Ran[a,1], Shuangbo Kong[b,c,1], Shuang Zhang[d,1], Jianghong Cheng[e], Chan Zhou[a,c], Bo He[c,d], Qiliang Xin[a], John P. Lydon[f], Francesco J. DeMayo[g], Gen-Sheng Feng[h], Guoliang Xia[a], Zhongxian Lu[e,2], Chao Wang[a,2], and Haibin Wang[b,c,2]

[a]State Key Laboratory of Agrobiotechnology, College of Biological Sciences, China Agricultural University, Beijing 100193, People's Republic of China; [b]Reproductive Medical Center, The First Affiliated Hospital of Xiamen University, Xiamen, Fujian 361003, People's Republic of China; [c]Fujian Provincial Key Laboratory of Reproductive Health Research, Medical College of Xiamen University, Xiamen, Fujian 361102, People's Republic of China; [d]State Key Laboratory of Stem Cell and Reproductive Biology, Institute of Zoology, University of Chinese Academy of Sciences, Chinese Academy of Sciences, Beijing 100101, People's Republic of China; [e]School of Pharmaceutical Sciences, State Key Laboratory of Cellular Stress Biology, Xiamen University, Xiamen, Fujian 361005, People's Republic of China; [f]Department of Molecular and Cellular Biology, Baylor College of Medicine, Houston, TX 77030; [g]Pregnancy and Female Reproduction Group, National Institute of Environmental Health Sciences, Research Triangle Park, NC 27709; and [h]Department of Pathology, Division of Biological Sciences, University of California, San Diego, La Jolla, CA 92093-0864

Edited by R. Michael Roberts, University of Missouri, Columbia, MO, and approved March 24, 2017 (received for review January 18, 2017)

Estrogen and progesterone coupled with locally produced signaling molecules are essential for embryo implantation. However, the hierarchical landscape of the molecular pathways that governs this process remains largely unexplored. Here we show that the protein tyrosine phosphatase Shp2, a positive transducer of RTK signaling, is predominately localized in the nuclei in the periimplantation mouse uterus. Uterine-specific deletion of Shp2 exhibits reduced progesterone receptor (PR) expression and progesterone resistance, which derails normal uterine receptivity, leading to complete implantation failure in mice. Notably, the PR expression defects are attributed to the limited estrogen receptor α (ERα) activation in uterine stroma. Further analysis reveals that nuclear Shp2, rather than cytosolic Shp2, promotes the ERα transcription activity. This function is achieved by enhancing the Src kinase-mediated ERα tyrosine phosphorylation, which facilitates ERα binding to *Pgr* promoter in an ERK-independent manner in periimplantation uteri. Besides uncovering a regulatory mechanism, this study could be clinically relevant to dysfunctional ERα-caused endometrial disorders in women.

Shp2 | ERK signaling | Src kinase | estrogen receptor | uterine receptivity

Successful implantation requires synchronization between an implantation-competent blastocyst and a receptive uterus. In humans, natural conception per cycle is poor (~30%), and ~75% of failed pregnancies are considered to be due to implantation failure (1). One-third of implantation failure is attributed to the embryo itself, whereas the remaining two-thirds appear to result from inadequate uterine receptivity (2). The endometrium enters into a receptive stage for blastocyst implantation only in a restricted time period termed "implantation window," which is dominated by precisely regulated proliferation and differentiation of endometrial epithelium and stroma under the influence of progesterone and estrogen (3).

Estrogen and progesterone bind to the estrogen receptor (ER) and progesterone receptor (PR), respectively, coupled with specific cofactors to endure the optimal functions. The activity of these nuclear receptors is also regulated at the posttranslational level by various modifications, such as phosphorylation, which can influence the protein stability, interaction with the cofactors and DNA binding affinity. So far, a wide range of nuclear receptor cofactors have been identified to ensure the normal ER transcriptional activation, such as the well-known steroid receptor coactivator (SRC) family members, which bind with ERα in the chromatin to recruit the histone acetyltransferase p300 (P300) for transcriptional activation (4–6). It is conceivable that ordered and combinatorial recruitment of cofactors at a specific target promoter after ERα binding to DNA sequence was essential to ensure target gene transcription. Recent evidence shows that nuclear receptor coactivator 6 is essential for embryo implantation by maintaining the appropriate level and activity of uterine ERα. Its deficiency induces aberrantly increased ERα protein level and thus hyperactivation of estrogen–ER signaling (7). Because either hyper- or hypoactivation of estrogen–ER signaling is associated with pregnancy disorders, such as recurrent implantation failure and endometriosis in women, it is extremely important to further explore the underlying mechanism governing normal ER transcriptional activation in the uterus during early pregnancy.

Src homology 2 domain containing protein tyrosine phosphatase (SHP2), encode by the gene *Ptpn11*, is a ubiquitously expressed protein tyrosine phosphatase, and its dysregulation is associated with malignant neoplasms and developmental disorders (8, 9).

Significance

Dysfunctional uterine receptivity is responsible for approximately 70% of implantation failures. This periimplantation event is dominated by ovarian hormones progesterone and estrogen functioning through their corresponding receptors, PR and ER, coupled with locally produced signaling molecules. However, the hierarchical landscape of the molecular pathways that govern this process remains largely unexplored. Here we show that Shp2, a classic cytoplasmic protein, is mainly located in the nuclei in uterine cells at periimplantation. Further investigation revealed that nuclear Shp2 enhances the Src kinase-mediated ERα tyrosine phosphorylation, facilitates ERα binding to *Pgr* promoter, and thus promotes the ERα transcription activity in periimplantation uteri. Our findings have high clinical significance in identifying novel therapeutic targets for the aberrant uterine receptivity and implantation failure.

Author contributions: H.R., S.K., S.Z., G.X., Z.L., C.W., and H.W. designed research; H.R., S.K., S.Z., J.C., C.Z., B.H., and Q.X. performed research; J.P.L., F.J.D., and G.-S.F. contributed new reagents/analytic tools; H.R., S.K., S.Z., G.X., Z.L., C.W., and H.W. analyzed data; and H.R., S.K., S.Z., C.W., and H.W. wrote the paper.

The authors declare no conflict of interest.

This article is a PNAS Direct Submission.

[1]H.R., S.K., and S.Z. contributed equally to this work.

[2]To whom correspondence may be addressed. Email: haibin.wang@vip.163.com, zhongxian@xmu.edu.cn, or wangcam@cau.edu.cn.

This article contains supporting information online at www.pnas.org/lookup/suppl/doi:10.1073/pnas.1700978114/-/DCSupplemental.

Structurally, Shp2 contains two N-terminally located Src-homology 2 domains (N-SH2 and C-SH2), a central phosphotyrosine phosphatase (PTP) domain and a C-terminal tail with tyrosyl phosphorylation sites and a proline-rich motif. Shp2 has been well defined as a positive cytoplasmic regulator for receptor protein tyrosine kinases (RTKs) in mediating cellular response to hormones, growth factors, and cytokines. Systemic deletion of Shp2 in mice results in embryonic lethality shortly after implantation, due to defective extracellular signal-regulated kinase (ERK) activation and the resulted death of trophoblast stem cells (10). However, it remains largely unknown whether uterine Shp2 is physiologically involved in regulating early pregnancy events. Because various RTK-coupled cytokines and growth factors, such as leukemia inhibitory factor (11), Interleukin 11 (12), and EGF family growth factors (13, 14), are essential for normal embryo implantation, we speculated that Shp2 could be an important player in directing normal early pregnancy events.

In the current study, using multiple genetic and molecular approaches, we provided strong evidence that Shp2 is essential for normal uterine receptivity and embryo implantation in an unexpected ERK-independent manner. Uterine-specific deletion of Shp2 dramatically limits estrogen receptor ERα transcriptional activity, leading to impaired uterine receptivity and complete implantation failure. In searching for the underlying molecular causes, we were surprised to find that nuclear Shp2 promotes ERα transcription activity by enhancing the Src kinase-mediated ERα tyrosine phosphorylation, which facilitates ERα binding to *Pgr* promoter in the periimplantation uteri.

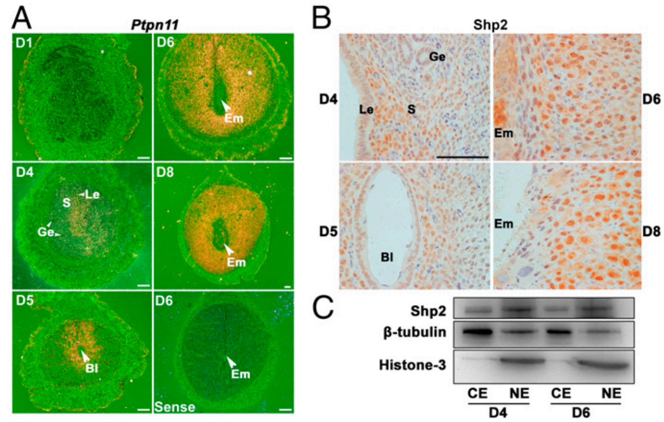

Fig. 1. Shp2 is spatiotemporally expressed in periimplantation mouse uteri exhibiting a nuclear localization. (*A*) In situ hybridization of *Ptpn11* mRNA in D1–4 uteri and D5–8 implantation sites. Shp2 mRNA is visible as the brown color. The white arrowhead indicates the embryo. (White scale bars, 250 μm.) (*B*) Immunohistochemical staining of Shp2 protein in D4 uteri and D5–8 implantation sites. The brown color indicates positive staining for Shp2. Note the dominant nuclear location of Shp2. (Black scale bar, 100 μm.) (*C*) Immunoblotting analysis of Shp2 protein in different cellular fractions from the D4 uteri and D6 implantation sites. β-Tubulin serves as a cytoplasmic loading control, whereas histone 3 serves as a nuclear loading control. Bl, blastocyst; CE, cytoplasmic extraction; Em, embryo; Ge, glandular epithelium; Le, luminal epithelium; NE, nuclear extraction; S, stroma. Data shown are representative of at least three independent experiments.

Results

Shp2 Exhibits Nuclear Localization in Mouse Uteri at Periimplantation. To address the pathophysiological significance of Shp2 during early pregnancy, we first examined mouse uterine expression pattern of Shp2 at periimplantation stage. As revealed by in situ hybridization, whereas *Ptpn11* was nearly undetectable in the uterus on day 1 of pregnancy (D1, day 1 = vaginal plug positive), its expression was intensely observed in subepithelial stromal cells on D4 (Fig. 1*A*). With the onset of embryo implantation on D5, *Ptpn11* was highly up-regulated in both the epithelial and stromal cells around the implanting blastocyst (Fig. 1*A*). With the initiation and progression of decidualization on D6–8, *Ptpn11* expression expanded into the entire decidual bed (Fig. 1*A*). This dynamic expression pattern suggests that Shp2 could be an important player during the periimplantation stage.

We next analyzed Shp2 protein distribution in periimplantation uteri by immunohistochemistry analysis. Consistent with its RNA expression pattern, Shp2 protein was highly expressed in uterine stroma (Fig. 1*B*). It was worthy to note that Shp2 was also localized to nuclei in proliferating and decidualizing stromal cells on D4–8 of pregnancy (Fig. 1*B*). This finding was further confirmed by the Western blot analysis showing a higher Shp2 expression in nuclear extracts (Fig. 1*C*). These observations point toward a potential nuclear-related function of Shp2 in the uterus during early pregnancy.

Uterine Shp2 Deficiency Completely Blocks Embryo Implantation Resulting in Female Infertility. To explore the uterine function of Shp2 at periimplantation, a mouse model harboring a uterine-specific deletion of Shp2 (*Shp2$^{d/d}$*) was generated by crossing Shp2-loxp mice (Shp2$^{f/f}$) with PR-Cre mice (*Pgr*$^{Cre/+}$). As illustrated in Fig. 2 *A*–*C*, Shp2 was efficiently deleted in PR-expressing uterine cells of *Shp2$^{d/d}$* females. No pups were found in vaginal plug-positive *Shp2$^{d/d}$* mice after mating with fertile wild-type (WT) males (Fig. 2*D*), demonstrating that the uterine depletion of Shp2 caused a complete infertile phenotype. To identify the stage-specific defects through pregnancy in *Shp2$^{d/d}$* females, early pregnancy events, including ovulation and implantation, were examined accordingly. On D1, all *Shp2$^{d/d}$* mice ovulated comparable numbers of oocytes as *Shp2$^{f/f}$* females (Fig. 2*E*). However, on D5–6, whereas *Shp2$^{f/f}$* mice displayed normal attachment reaction as visible by blue dye injection, none of *Shp2$^{d/d}$* mice showed signs of implantation and unimplanted blastocysts with normal morphology can be recovered from the *Shp2$^{d/d}$* uteri (Fig. 2 *F*–*H*). These results clearly indicate that uterine Shp2 is indispensable for normal embryo implantation.

Shp2 Depletion Derails Normal Uterine Receptivity Depicting Progesterone Resistance. To portray the uterine lumen morphology at periimplantation, we performed immunofluorescence staining of cytokeratin (an epithelial marker) and Ki-67 (a cell proliferation marker). We observed that *Shp2$^{d/d}$* uteri exhibited a defective luminal closure characterized by increased uterine epithelial branches (Fig. 3*A*). Moreover, Ki-67 staining analysis revealed an aberrant epithelial proliferation accompanied by a dramatically decreased stromal cell division in *Shp2$^{d/d}$* mice (Fig. 3 *B* and *C*). These cellular defects indicate an abnormal uterine receptivity upon Shp2 deficiency.

Because progesterone and estrogen are the principle determinants of uterine receptivity in mice, we next measured serum levels of progesterone (P_4) and estradiol-17β (E_2) in D4 *Shp2$^{f/f}$* and *Shp2$^{d/d}$* female mice. As shown in Fig. S1 *A* and *B*, we observed comparable circulating levels of E_2 and a slight decreased level of P_4. Immunohistochemistry staining revealed that the corpus luteum expressed lower levels of Shp2 in comparison with the developing follicles (Fig. S1*C*). However, depletion of luteal Shp2 exerted no apparent influence on the expression of progesterone biosynthetic enzymes, cytochrome P450 cholesterol side-chain cleavage enzyme, and 3β-hydroxysteroid dehydrogenase II (Fig. S1*C*). To further test whether this slightly reduced progesterone secretion was the main cause for implantation failure in *Shp2$^{d/d}$* females, we supplied P_4 in the null mice for 3 consecutive days starting on D3. However, P_4 supplementation failed to restore embryo implantation in *Shp2$^{d/d}$* mice (Fig. S1*D*). This result indicates that implantation failure in *Shp2$^{d/d}$* mice is intrinsic to uterine dysfunctions.

PHYSIOLOGY

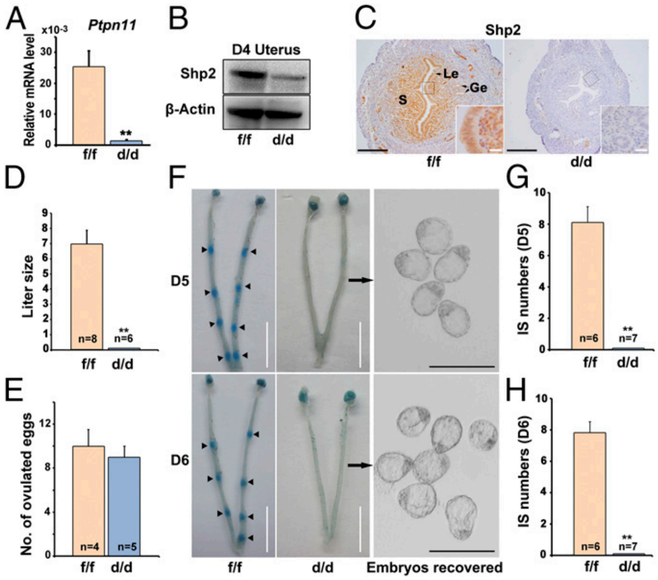

Fig. 2. Uterine Shp2 deficiency induces complete implantation failure resulting in female infertility. (*A*) Real-time PCR analysis of *Shp2* mRNA levels in D4 uteri from wild-type (*Shp2*$^{f/f}$) and knockout (*Shp2*$^{d/d}$) mice. The values are normalized to the *Gapdh* expression level and indicated as the mean ± SEM, $n = 3$. $^{**}P < 0.01$. (*B*) Immunoblotting analysis of Shp2 protein levels in D4 *Shp2*$^{f/f}$ and *Shp2*$^{d/d}$ uteri. β-Actin is used as loading control. (*C*) Immunohistochemistry analysis of Shp2 protein in D4 *Shp2*$^{f/f}$ and *Shp2*$^{d/d}$ uteri. Ge, glandular epithelium; Le, luminal epithelium; S, stroma. (White scale bar, 25 μm; black scale bar, 250 μm.) (*D*) Average litter sizes in *Shp2*$^{f/f}$ and *Shp2*$^{d/d}$ female mice. Number within the bar indicated the number of mice tested. $^{**}P < 0.01$. (*E*) Number of ovulated oocytes in *Shp2*$^{f/f}$ and *Shp2*$^{d/d}$ mice. Number within the bar indicates the number of mice tested. (*F*) Implantation status of *Shp2*$^{f/f}$ and *Shp2*$^{d/d}$ mice on D5–6. Implantation sites are visualized by blue dye method and the unimplanted embryos are recovered from *Shp2*$^{d/d}$ uteri (*Right* image). Black arrowheads indicate the implantation sites. Black arrows indicate the embryos in the right panels are recovered from the corresponding uteri. (White scale bar, 1 cm; black scale bar, 250 μm.) (*G* and *H*) Average number of implantation sites in *Shp2*$^{f/f}$ and *Shp2*$^{d/d}$ mice on D5 (*G*) and D6 (*H*) of pregnancy. Number within the bar indicates the number of mice tested. Mice that failed to recover any embryos are excluded in statistical analysis. IS, implantation site; $^{**}P < 0.01$. Data shown are representative of at least four independent experiments.

To reveal the molecular basis of phenotypic defects in the absence of uterine Shp2, we then analyzed the expression of implantation-related genes in D4 uteri by qPCR and in situ hybridization. As shown in Fig. 3 *D* and *E*, whereas the epithelial estrogen-regulated genes including mucin 1 (*Muc1*) and lactotransferrin (*Ltf*) were aberrantly induced in *Shp2*$^{d/d}$ mice, all progesterone-targeting genes, such as amphiregulin (*Areg*), homeobox A10 (*Hoxa10*), heart and neural crest derivatives expressed 2 (*Hand2*), and chicken ovalbumin upstream promoter transcription factor 2 (*Coup-tfII*, also known as *Nr2f2*) were down-regulated in *Shp2*$^{d/d}$ uteri. This abnormal expression profile of implantation-related genes was well coincident with abnormal epithelial versus stromal proliferation (Fig. 3 *B* and *C*), indicating an impaired progesterone activity and loss of antagonistic influence of progesterone–PR signaling on estrogen-stimulated epithelial proliferation in *Shp2*$^{d/d}$ uteri. However, this molecular and cellular abnormality was not due to above-mentioned reduced circulating progesterone level, because progesterone supplementation failed to restore normal uterine receptivity marker gene expression (Fig. S1*E*) and uterine epithelial versus stromal proliferation in *Shp2*$^{d/d}$ uteri (Fig. S1*F*). Similar observation of enhanced uterine epithelial proliferation with reduced stromal proliferation can be mimicked in *Shp2*$^{f/f}$ mice by the treatment of progesterone antagonist RU486 (Fig. S2), phenocopying the progesterone resistance in mice lacking uterine Shp2.

Loss of Shp2 Compromises Uterine Estrogen Responsiveness and thus PR Expression Independent of ERK Pathway. To reveal the underlying causes of progesterone resistance in *Shp2*$^{d/d}$ mice, we next analyzed ERα and PR expression in D4 *Shp2*$^{f/f}$ and *Shp2*$^{d/d}$ uteri. As shown in Fig. 4 *A*–*C*, ERα was comparably expressed even in the absence of uterine Shp2. In contrast, the expression of PR (encoded by *Pgr*) was significantly decreased in *Shp2*$^{d/d}$ uteri. Further localization analysis revealed that the stroma PR was severely decreased in *Shp2*$^{d/d}$ uteri (Fig. 4*D*). As the stroma *Pgr* is induced by the estrogen–ER signaling, to explore whether this decreased *Pgr* expression is due to hampered estrogen activities, we further analyzed some other ER target genes, including insulin-like growth factor 1 (*Igf1*) and erythroblastosis oncogene B 1 (*Erbb1*). They also displayed decreased expression in the *Shp2*$^{d/d}$ uteri (Fig. 4*D*). This interesting finding suggests that progesterone resistance from Shp2 deficiency is secondary to impaired uterine responsiveness to estrogen, regardless of normal circulating estrogen level and uterine ERα expression in null mice.

To further confirm that this reduced PR expression in uterine stroma was due to hampered estrogen activities upon Shp2 deletion, we used an ovariectomized mouse model. As illustrated in Fig. 4*E*, all tested ER target genes, including *Pgr*, *Igf1*, vascular endothelial growth factor (*Vegf*), and *Erbb1* were expressed at significantly lower levels at 6 h after estrogen challenge in ovariectomized *Shp2*$^{d/d}$ uteri compared with that in *Shp2*$^{f/f}$ females. In situ hybridization analysis further revealed that the induction of ER-targeting gene-like *Pgr* was not noted in *Shp2*$^{d/d}$ stroma after estrogen stimulation (Fig. 4*F*). These results reinforce the notion that Shp2 deficiency compromises uterine estrogen responsiveness and thus its target gene expression including *Pgr* in uterine stroma.

Because Shp2 is known as a positive signal transducer in ERK pathway, to test whether Shp2 would function through ERK pathway to regulate ERα activity in the uterus, we next examined the expression of p-ERK1/2 (activated form of ERK1/2) in D4 *Shp2*$^{f/f}$ and *Shp2*$^{d/d}$ uteri. Unexpectedly, p-ERK1/2 levels remained unaltered in *Shp2*$^{d/d}$ uteri (Fig. S3 *A* and *B*), suggesting that Shp2 may function through an ERK-independent manner to

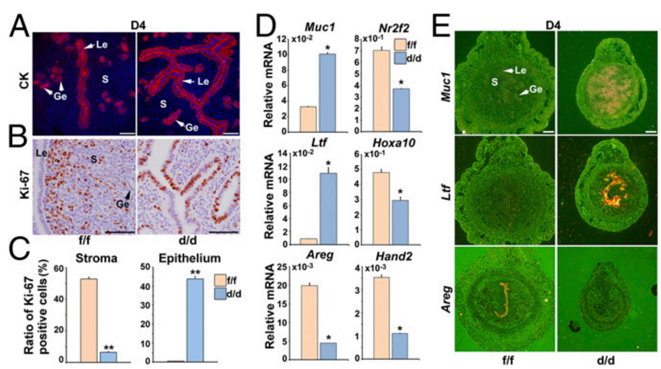

Fig. 3. Shp2 depletion derails normal uterine receptivity depicting progesterone resistance. (*A*) Immunofluorescence staining of cytokeratin (CK) in D4 *Shp2*$^{f/f}$ and *Shp2*$^{d/d}$ uteri. Cy3-labeled antigen is showed in red, whereas Hoechst 33342 labeled the nuclei as blue. (Scale bars, 200 μm.) (*B*) Immunohistochemical staining of Ki-67 in D4 *Shp2*$^{f/f}$ and *Shp2*$^{d/d}$ uteri. The brown color indicates the positive signal. (Scale bars, 100 μm.) (*C*) Quantitative analysis of Ki-67 positive cells in D4 *Shp2*$^{f/f}$ and *Shp2*$^{d/d}$ uteri. $^{**}P < 0.01$. (*D*) Real-time PCR analysis of the implantation-related marker gene expression in D4 *Shp2*$^{f/f}$ and *Shp2*$^{d/d}$ uteri. The values are normalized to the *Gapdh* expression level and indicated as the mean ± SEM, $n = 3$. $^{*}P < 0.05$. (*E*) In situ hybridization of *Ltf*, *Muc1*, and *Areg* in D4 *Shp2*$^{f/f}$ and *Shp2*$^{d/d}$ uteri. The brown color indicates the positive signal. Ge, glandular epithelium; Le, luminal epithelium; S, stroma. (Scale bars, 250 μm.) Data shown are representative of at least three independent experiments.

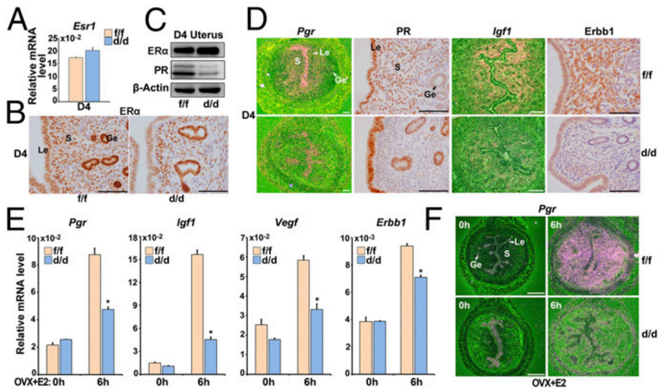

Fig. 4. Loss of Shp2 compromises uterine estrogen responsiveness and thus PR expression. (*A*) Real-time PCR detection of the mRNA levels of *Esr1* in D4 *Shp2*$^{f/f}$ and *Shp2*$^{d/d}$ uteri. The values are normalized to the *Gapdh* expression level and indicated as the mean ± SEM, $n = 3$. (*B*) Immunohistochemical staining of ERα in D4 *Shp2*$^{f/f}$ and *Shp2*$^{d/d}$ uteri. The brown color indicates the positive signal. (*C*) Immunoblotting analysis of ERα and PR in D4 *Shp2*$^{f/f}$ and *Shp2*$^{d/d}$ uteri. β-Actin is used as loading control. (*D*) In situ hybridization and immunohistochemical analysis of estrogen–ERα target genes in D4 *Shp2*$^{f/f}$ and *Shp2*$^{d/d}$ uteri. The brown color indicates the positive signal. (*E*) Real-time PCR detection of estrogen–ERα target gene expression levels in *Shp2*$^{f/f}$ and *Shp2*$^{d/d}$ ovariectomized mouse uteri in response to E_2 treatment. The values are normalized to the *Gapdh* expression level and indicated as the mean ± SEM, $n = 3$. *$P < 0.05$. (*F*) In situ hybridization of *Pgr* in *Shp2*$^{f/f}$ and *Shp2*$^{d/d}$ ovariectomized mouse uteri after E_2 treatment. The brown color indicates the positive signal. Ge, glandular epithelium; Le, luminal epithelium; S, stroma. (White scale bar, 250 μm; black scale bar, 100 μm.) Data shown are representative of at least three independent experiments.

ensure ER activation during uterine receptivity establishment. To further exclude the possibility that Shp2 ensure the ERα activity via ERK pathway, we treated the human endometrial Ishikawa cells with a specific MEK1/2 inhibitor, U0126. The data demonstrated that ERK inhibition exerts apparently no influence on ERα transcriptional activation, because E_2 can significantly induce ER-targeting gene *PGR* expression even in the presence of U0126 (Fig. S3*C*).

Nuclear Shp2 Rather than Cytosolic Shp2 Is Required for Normal ERα Activation. To further delineate the molecular basis of Shp2 on ERα, we next used a human endometrial Ishikawa cell line for in vitro study. Because Ishikawa cells expressed high levels of endogenous SHP2 (Fig. 5 *A* and *B*), we generated a *SHP2* null mutant Ishikawa cell line by CRISPR/Cas9 strategy (Fig. S4 *A*–*C*). As shown in Fig. 5 *A* and *B*, we found the expression of SHP2 was completely deleted in *SHP2* null cells. Besides, the ERK1/2 activation in response to amphiregulin (Areg) was also abolished in the knockout cells (Fig. S4*D*). Most importantly, *SHP2* deficiency in Ishikawa cells significantly hampered estrogen-induced target gene expression, such as *PGR* and *IGF1*, whereas transfection with the full-length wild-type SHP2 (SHP2-WT) can rescue this defect (Fig. 5*C*). These observations confirm the findings in *Shp2*$^{d/d}$ mouse uteri, proving that SHP2 is essential for normal ER transcriptional activity.

Because we observed a high level of Shp2 within the nucleus, to test whether the facilitating effect of Shp2 on ERα activation would depend on its nuclear localization, we next introduced a nucleus-excluded form of HA-tagged SHP2 (SHP2-NES) that contained a potent nuclear export sequence fused to the carboxyl terminus of original SHP2 (15). As expected, whereas the *SHP2* mutant Ishikawa cell line transfected with HA-labeled SHP2-WT exhibited both cytosolic and nuclear localization, the null mutant cells transfected with SHP2-NES showed prominent cytosolic accumulation of SHP2 (Fig. 5*D*). Furthermore, whereas ERK1/2 activation in response to amphiregulin (Areg) could be largely restored by both SHP2-NES and SHP2-WT in knockout Ishikawa cells (Fig. 5*E*), SHP2-NES, unlike SHP2-WT, failed to rescue E_2-induced ERE (estrogen-responsive element) response in mutant cells (Fig. 5*F*). These findings indicate that nuclear Shp2 rather than cytosolic Shp2 is required for normal ERα activity.

Nuclear Shp2 Enhances ERα Phosphorylation via Src Kinase Activation, Facilitating Its Binding to *Pgr* Promoter. Because ERα and Shp2 both exhibited nuclear localization in the uterus, we tested the possibility of whether Shp2 could interact with ERα. Coimmunoprecipitation analysis revealed that Shp2 can physically interact with ERα in D4 receptive uteri as well as in Ishikawa cells (Fig. 6 *A* and *B*). To further define which part of SHP2 mediated the interaction with ERα, we generated truncation mutants of SHP2 harboring PTP domain deletion (ΔPTP) or SH2 domain deletions (ΔSH2). Using coimmunoprecipitation analysis, we found, whereas the ΔSH2 mutant containing PTP domain only exhibited barely detectable binding affinity with ERα, ΔPTP mutant with intact SH2 domains showed significantly higher binding affinity (Fig. 6*C*). These findings suggest that SH2 domains are the key regions physically interacting with ERα. However, neither the ΔSH2 nor ΔPTP could reverse the defective E_2–ER response in the absence of intact SHP2 (Fig. S5). The inability of inactive SHP2 with phosphatase point mutation to restore the E_2–ER response further suggests that the phosphatase activity of SHP2 is also critical for promoting the ER activity.

As a transcription factor, nuclear-located ERα would bind to the DNA of target genes, we wonder whether Shp2 would translocate to the chromatin with ERα. The whole cell lysates were fractionated into chromatin and soluble fractions. As shown in Fig. 6*D*, Shp2 was detected in the soluble compartment, but not in the chromatin fraction, whereas the ERα was positive both in the soluble and chromatin fractions. The ChIP–qPCR analysis further confirmed the absence of Shp2 in the chromatin fraction. There is no significant enrichment of Shp2 on the *Pgr* promotor

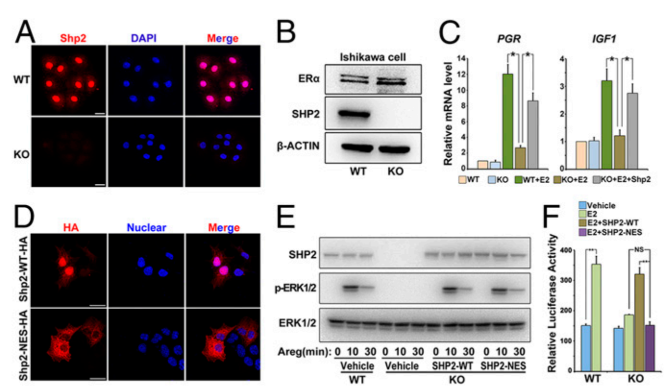

Fig. 5. Nuclear SHP2 is essential for normal ERα activation. (*A*) Immunofluorescence staining of SHP2 in WT and *SHP2* knockout (KO) Ishikawa cells. Cy3-labeled antigen is showed in red; DAPI labeled the nuclei as blue. (Scale bars, 25 μm.) (*B*) Immunoblotting analysis of SHP2 and ERα in WT and KO Ishikawa cell line. β-Actin serves as a control. (*C*) Real-time PCR detection of estrogen–ERα target genes *PGR* and *IGF1* in *SHP2* KO Ishikawa cells. The values are normalized to the *GAPDH* expression level and shown as the mean ± SEM, *$P < 0.05$, $n = 3$. (*D*) Immunofluorescence staining of HA-tagged SHP2 in *SHP2* knockout Ishikawa cell line transfected with the WT-SHP2 or NES-SHP2. The DAPI is used for nuclear staining. (Scale bars, 150 μm.) (*E*) Western blot analysis of p-ERK1/2 and total ERK1/2 after amphiregulin (Areg) treatment in *SHP2* WT and KO Ishikawa cell line transfected with different vectors as indicated. (*F*) ERE-luciferase reporter assay to evaluate the ERα activation in *SHP2* WT and KO cells transfected with HA-tagged wild-type or SHP2-NES vectors. The values are shown as the mean ± SEM, *$P < 0.05$, $n = 3$. Data shown are representative of at least three independent experiments. **$P < 0.01$. NS, no significance.

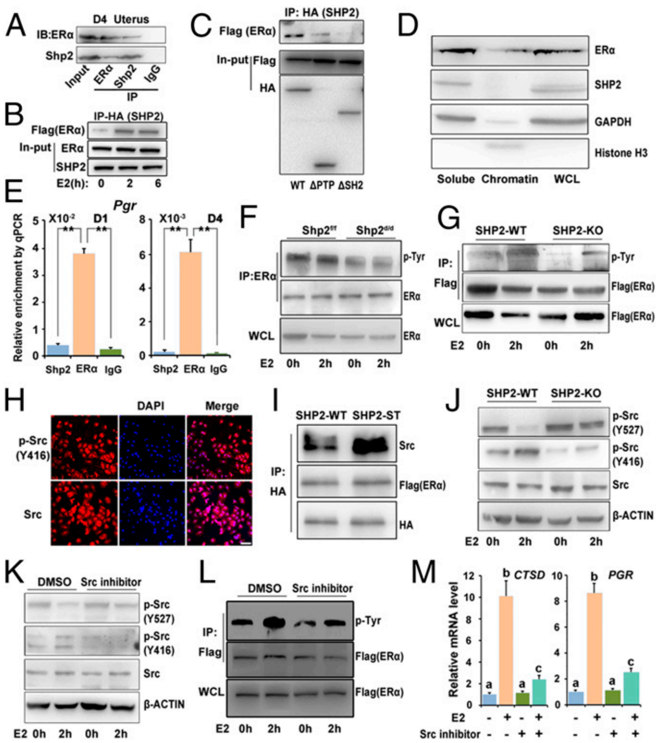

Fig. 6. Nuclear Shp2 enhances ERα phosphorylation via Src kinase activation. (*A*) Immunoprecipitation analysis to detect the interaction of endogenous Shp2 and ERα. D4 uterine tissue lysates were subjected to immunoprecipitation using an anti-ERα, anti-Shp2 antibody, or rabbit IgG, followed by immunoblotting with respective antibodies. (*B*) Immunoprecipitation analysis for detecting the association of exogenously expressed SHP2 (HA tagged) and ERα (Flag tagged). Cell lysis with or without E_2 treatment is immunoprecipitated by HA (SHP2) antibody and immunoblotted with the antibodies against Flag (ERα). (*C*) Immunoprecipitation analysis of the physical interaction of ERα with the different SHP2 mutants. Ishikawa cell lysates (cotransfection with Flag-tagged ERα vectors and HA-tagged wild-type or truncated SHP2 vectors) are subjected to immunoprecipitation by HA antibody, and the immunoprecipitates are then immunoblotted against the Flag antibody. (*D*) Immunoblot analysis of Shp2 and ER proteins in uterine cellular soluble or insoluble (chromatin) fraction. Whole cell lysate (WCL) was used as control. GAPDH is used as soluble fraction control and histone H3 as the chromatin fraction control. (*E*) ChIP–qPCR analysis for enrichment of Shp2 and ERα in the *Pgr* promotor in D1 and D4 uteri. The values are shown as the mean ± SEM, $n = 3$. $^{**}P < 0.01$. (*F* and *G*) Immunoblot analysis of ER Tyr phosphorylation in anti-ER immunoprecipitates by p-Tyr antibody. The cellular lyses are from the E_2-challenged ovariectomized mice (*F*) or in vitro cultured Ishikawa cells (*G*). (*H*) Immunofluorescence staining of total and active form of Src in Ishikawa cells. DAPI was used to stain the nuclear DNA. (Scale bar, 100 μm.) (*I*) Immunoblot analysis of indicated proteins in anti-HA (SHP2) immunoprecipitates. The cellular lyses for immunoprecipitation are from the Ishikawa cells transfected with the HA-tagged WT or substrate trapping (ST) Shp2 and Flag-tagged ERα. (*J*) Immunoblot analysis for detecting the phosphorylation level of Src in *SHP2* WT or KO Ishikawa cells with or without E_2 treatment; β-actin was used as loading control. (*K*) Immunoblot analysis for detecting phosphorylated Src in WT Ishikawa cells treated with Src inhibitor saracatinib or control DMSO for 2 h before the E2 challenge. (*L*) Immunoblot analysis of ER Tyr phosphorylation in anti-Flag (ERα) immunoprecipitates following the Src inhibitor treatment. (*M*) Real-time PCR analysis of E_2-induced gene in Ishikawa cells pretreated with Src inhibitor saracatinib. The values are normalized to the *GAPDH* expression level and shown as the mean ± SEM, $n = 4$. The different letters (*a*, *b*, and *c*) indicate significant differences between groups (*a* vs. *b* and *b* vs. *c*: $P < 0.01$; *a* vs. *c*: $P < 0.05$). Data shown are representative of at least three independent experiments. IP, immunoprecipitation.

compared with the IgG, whereas ERα indeed can bind within this element (Fig. 6*E*).

Next, we asked whether the Shp2 could influence the ER protein modification before the ERα recruitment to the DNA, particularly the ERα Tyr phosphorylation that has been reported to regulate the ERα activity (16). Because Shp2 is a protein tyrosine phosphatase, we speculated that Shp2 deficiency would lead to an increased Tyr phosphorylation of ERα in case ERα is a direct substrate of Shp2. By contrast, after E_2 challenge, a decreased Tyr phosphorylation level of ERα was observed both in vivo and in vitro in the absence of Shp2 (Fig. 6 *F* and *G* and Fig. S6 *A* and *B*), implying that ERα is not a direct substrate of Shp2, and there is another upstream kinase for ERα phosphorylation modification.

The phosphorylation of ERα has been reported to influence the ER binding to DNA and interaction with the cofactors such as SRC and P300. Indeed, the ChIP–qPCR analysis revealed that binding of ERα to *Pgr* promotor was severely dampened in the absence of Shp2 both in D4 uteri and E_2-challenged ovariectomized mouse uteri (Fig. S7 *A* and *B*). Moreover, even the cofactors SRC1 and P300 were normally expressed in the *Shp2* knockout uteri (Fig. S7*C*), the interaction between ERα and these cofactors was markedly reduced in the *Shp2* null uteri (Fig. S7*D*). These findings suggest that uterine Shp2 deficiency attenuates ERα Tyr phosphorylation, and decreases its recruitment to target genes and interaction with the cofactors, leading to impaired uterine estrogen responsiveness.

Because Src kinase was reported to influence the ERα Tyr phosphorylation, we thus examined the expression of Src and its activated phosphorylated form (p-Y416). As shown in Fig. 6*H*, the protein exhibited both the cytoplasmic and nuclear localization. Previous studies suggest that Shp2 promotes c-Src activation by directly or indirectly controlling phosphorylation of C-terminal inhibitory phosphorylation site Tyr527. We then used the substrate trapping strategy to define whether the Src kinase is a direct substrate of Shp2. Unlike ERα, the Src kinase preferentially interacted with the trapping mutant Shp2, suggesting the Src rather than ERα is a potential substrate of SHP2 phosphatase (Fig. 6*I*). Moreover, the inhibitory Y527 phosphorylation form of Src was more prominent in the *SHP2* knockout cells (Fig. 6*J*).

We then analyzed the consequence of Src kinase inhibition on ER activation. As shown in Fig. 6*K*, pretreatment with SRC inhibitor saracatinib abolished estrogen-evoked Src activation, as demonstrated by decreased level of pY416 and abnormal high level of inhibitory Y527 phosphorylation. This inhibitor pretreatment also substantially impaired the ERα Tyr phosphorylation (Fig. 6*L*). Moreover, Src kinase inhibition also abolished the E_2-induced target gene expression (Fig. 6*M*), faithfully mimicking the *Shp2* knockout phenotype. Together, these data support the notion that Shp2 promotes the ERα transcriptional activity by enhancing the Src kinase-mediated ERα tyrosine phosphorylation.

Discussion

In our study, we observed a dramatically decreased PR expression in the stroma in the absence of uterine Shp2, associated with attenuated stromal growth and aberrant epithelial overproliferation, indicating that Shp2 is essential for normal stromal PR expression and epithelial–stromal interactions during uterine transformation for receptivity. This observation is consistent with previous observations that insufficient PR signaling hampers the intimate stromal–epithelial crosstalk and thus uterine receptivity (17, 18). However, it was a meandering path for us to realize and confirm that this functional progesterone resistance in the absence of uterine Shp2 is seeded by the significantly decreased level of stromal PR protein, which results from an impaired estrogen–ERα activity in stroma. It is also worthy to note that the epithelial estrogen–ER signaling seems normal, which is consistent with the low expression level of Shp2 in epithelium. This finding suggests a cell context-specific function of Shp2 in ensuring the ERα activity and/or the disappearance of stromal PR antagonistic influence. Meanwhile, there is no apparent decrease of epithelial PR expression in $Shp2^{d/d}$ uteri at periimplantation, confirming the hampered ER activity in the absence of Shp2, because it is the stroma estrogen–ERα signaling that suppresses the epithelial PR expression (19).

In searching for the underlying molecular mechanisms, we further demonstrate that Shp2 in the nucleus can enhance the Src kinase-mediated ERα tyrosine phosphorylation, facilitate ERα binding to target gene promoter, and thus promote the ERα transcription activity in periimplantation uteri (Fig. S8). In fact, there was evidence showing that Shp2 can translocate into the nucleus to participate in DNA damage-induced apoptotic responses (20, 21), forming a complex with STAT5 for regulation of target gene transcription (22) or interacting with telomerase reverse transcriptase involved in replicative senescence (23). Most recent studies also showed that nuclear Shp2 can dephosphorylate parafibromin influencing Wnt targeting-gene activation (24, 25). In our study, we found that Shp2 mainly functions in the nucleus in an enzyme activity-dependent way and interacts with the ERα mainly through SH2 domain. However, this interaction is not equivalent to enzyme–substrate interaction and therefore does not necessarily suggest that ER is a substrate candidate of Shp2. Indeed, the Shp2 enhances the Tyr phosphorylation of ER by facilitating the Src kinase activity through dephosphorylation of an inhibitory Tyr in Src kinase. Whereas the Src kinase is broadly recognized as a cytoplasmic protein, recent reports also observed the nuclear function of this kinase that was activated by Shp2 through dephosphorization of the inhibitory p-Tyr site for DNA damage response (26).

Nonetheless, besides uncovering a function and mechanism of nuclear Shp2 in ensuring normal ERα transcriptional activation conducive to uterine receptivity and implantation, our findings have high clinical significance, because dysfunctional ERα activity is often associated with multiple endometrial disorders.

Materials and Methods

Animals and Treatments. *Shp2$^{flox/flox}$* mice were generated as previously described (27). Uterine-specific knockout mice were generated by crossing *Shp2$^{flox/flox}$* mice with *Pgr$^{Cre/+}$* mice. All mice were housed in the animal care facility of Xiamen University, in accordance with the guidelines for the care and use of laboratory animals. Experimental procedures to treat mice and analyze implantation sites are provided in *SI Materials and Methods*.

In Situ Hybridization. In situ hybridization was performed as previously described (28). Sections hybridized with the sense probes served as negative controls. Mouse-specific cRNA probes for *Ptpn11*, *Ltf*, *Muc1*, *Areg*, *Pgr*, and *Igf1* were used for hybridization.

Immunostaining. Immunohistochemistry and immunofluorescence analysis were performed as described previously (29).

Western Blot. Protein extraction and Western blot analysis were performed as described previously (28). Insoluble chromatin fraction and soluble fraction were extracted according to the previous methods (30). Uncropped images of immunoblots are provided in Fig. S9.

Real-Time RT-PCR Analysis. Quantitative RT-PCR was performed as described (31). All primers for real-time PCR are listed in Table S1. All real-time PCR experiments were repeated at least three times.

Generation of *SHP2* Knockout Human Ishikawa Cell Line. Ishikawa cells were maintained at 37 °C in an atmosphere of 5% CO_2/95% air in DMEM supplemented with 10% (vol/vol) FBS. *SHP2*-deficient Ishikawa cells were generated by CRISPR/Cas9-mediated genome engineering.

Coimmunoprecipitation and Chromatin Immunoprecipitation. Coimmunoprecipitation (co-IP) and chromatin immunoprecipitation (ChIP) analysis were performed as previously described (31). Immunoprecipitated proteins were separated by SDS/PAGE and detected by immunoblotting using the respective antibodies. Specific primers were used to detect immunoprecipitated chromatin fragments, as well as input chromatin (Table S1).

Statistical Analysis. All data are presented as mean ± SEM. Each experiment included at least three independent samples. Comparison between two groups was made by unpaired Student's two-tailed *t* test, and comparisons among three groups or more were made by one-way ANOVA test. $P < 0.05$ was considered to indicate a significant result.

ACKNOWLEDGMENTS. We thank Xiaofang Tang for her assistance in immunoblot analysis. This work was supported in parts by the National Natural Science Foundation (81130009, 81330017, and 81490744 to H.W.; 81601285 to S.K.; and 31471106 to S.Z.).

1. Norwitz ER, Schust DJ, Fisher SJ (2001) Implantation and the survival of early pregnancy. *N Engl J Med* 345:1400–1408.
2. Achache H, Revel A (2006) Endometrial receptivity markers, the journey to successful embryo implantation. *Hum Reprod Update* 12:731–746.
3. Wang H, Dey SK (2006) Roadmap to embryo implantation: Clues from mouse models. *Nat Rev Genet* 7:185–199.
4. Xu J, et al. (1998) Partial hormone resistance in mice with disruption of the steroid receptor coactivator-1 (SRC-1) gene. *Science* 279:1922–1925.
5. Suen CS, et al. (1998) A transcriptional coactivator, steroid receptor coactivator-3, selectively augments steroid receptor transcriptional activity. *J Biol Chem* 273:27645–27653.
6. Xu J, et al. (2000) The steroid receptor coactivator SRC-3 (p/CIP/RAC3/AIB1/ACTR/TRAM-1) is required for normal growth, puberty, female reproductive function, and mammary gland development. *Proc Natl Acad Sci USA* 97:6379–6384.
7. Kawagoe J, et al. (2012) Nuclear receptor coactivator-6 attenuates uterine estrogen sensitivity to permit embryo implantation. *Dev Cell* 23:858–865.
8. Mohi MG, Neel BG (2007) The role of Shp2 (PTPN11) in cancer. *Curr Opin Genet Dev* 17:23–30.
9. Grossmann KS, Rosário M, Birchmeier C, Birchmeier W (2010) The tyrosine phosphatase Shp2 in development and cancer. *Adv Cancer Res* 106:53–89.
10. Yang W, et al. (2006) An Shp2/SFK/Ras/Erk signaling pathway controls trophoblast stem cell survival. *Dev Cell* 10:317–327.
11. Stewart CL, et al. (1992) Blastocyst implantation depends on maternal expression of leukaemia inhibitory factor. *Nature* 359:76–79.
12. Robb L, et al. (1998) Infertility in female mice lacking the receptor for interleukin 11 is due to a defective uterine response to implantation. *Nat Med* 4:303–308.
13. Xie H, et al. (2007) Maternal heparin-binding-EGF deficiency limits pregnancy success in mice. *Proc Natl Acad Sci USA* 104:18315–18320.
14. Large MJ, et al. (2014) The epidermal growth factor receptor critically regulates endometrial function during early pregnancy. *PLoS Genet* 10:e1004451.
15. Li B, et al. (2014) Fructose-1,6-bisphosphatase opposes renal carcinoma progression. *Nature* 513:251–255.
16. Sun J, Zhou W, Kaliappan K, Nawaz Z, Slingerland JM (2012) ERα phosphorylation at Y537 by Src triggers E6-AP-ERα binding, ERα ubiquitylation, promoter occupancy, and target gene expression. *Mol Endocrinol* 26:1567–1577.
17. Lee K, et al. (2006) Indian hedgehog is a major mediator of progesterone signaling in the mouse uterus. *Nat Genet* 38:1204–1209.
18. Tranguch S, et al. (2005) Cochaperone immunophilin FKBP52 is critical to uterine receptivity for embryo implantation. *Proc Natl Acad Sci USA* 102:14326–14331.
19. Kurita T, et al. (2000) Paracrine regulation of epithelial progesterone receptor by estradiol in the mouse female reproductive tract. *Biol Reprod* 62:821–830.
20. Yuan L, Yu WM, Yuan Z, Haudenschild CC, Qu CK (2003) Role of SHP-2 tyrosine phosphatase in the DNA damage-induced cell death response. *J Biol Chem* 278:15208–15216.
21. Yuan L, Yu WM, Xu M, Qu CK (2005) SHP-2 phosphatase regulates DNA damage-induced apoptosis and G2/M arrest in catalytically dependent and independent manners, respectively. *J Biol Chem* 280:42701–42706.
22. Chughtai N, Schimchowitsch S, Lebrun JJ, Ali S (2002) Prolactin induces SHP-2 association with Stat5, nuclear translocation, and binding to the beta-casein gene promoter in mammary cells. *J Biol Chem* 277:31107–31114.
23. Jakob S, et al. (2008) Nuclear protein tyrosine phosphatase Shp-2 is one important negative regulator of nuclear export of telomerase reverse transcriptase. *J Biol Chem* 283:33155–33161.
24. Takahashi A, et al. (2011) SHP2 tyrosine phosphatase converts parafibromin/Cdc73 from a tumor suppressor to an oncogenic driver. *Mol Cell* 43:45–56.
25. Tsutsumi R, et al. (2013) YAP and TAZ, Hippo signaling targets, act as a rheostat for nuclear SHP2 function. *Dev Cell* 26:658–665.
26. Liu X, et al. (2016) Gain-of-function mutations of Ptpn11 (Shp2) cause aberrant mitosis and increase susceptibility to DNA damage-induced malignancies. *Proc Natl Acad Sci USA* 113:984–989.
27. Zhang EE, Chapeau E, Hagihara K, Feng GS (2004) Neuronal Shp2 tyrosine phosphatase controls energy balance and metabolism. *Proc Natl Acad Sci USA* 101:16064–16069.
28. Wang Q, et al. (2013) Wnt6 is essential for stromal cell proliferation during decidualization in mice. *Biol Reprod* 88:5.
29. Lu J, et al. (2013) A positive feedback loop involving Gcm1 and Fzd5 directs chorionic branching morphogenesis in the placenta. *PLoS Biol* 11:e1001536.
30. Wu L, Li L, Zhou B, Qin Z, Dou Y (2014) H2B ubiquitylation promotes RNA Pol II processivity via PAF1 and pTEFb. *Mol Cell* 54:920–931.
31. Zhang S, et al. (2014) Uterine Rbpj is required for embryonic-uterine orientation and decidual remodeling via Notch pathway-independent and -dependent mechanisms. *Cell Res* 24:925–942.